Fisher Matrix Optimization of Cosmic Microwave Background Interferometers

Haonan Liu* and Emory F. Bunn
Physics Department, University of Richmond, Richmond, VA 23173

We describe a method for forecasting errors in interferometric measurements of polarization of the cosmic microwave background (CMB) radiation, based on the use of the Fisher matrix calculated from the visibility covariance and relation matrices. In addition to noise and sample variance, the method can account for many kinds of systematic error by calculating an augmented Fisher matrix, including parameters that characterize the instrument along with the cosmological parameters to be estimated. The method is illustrated with examples of gain errors and errors in polarizer orientation. The augmented Fisher matrix approach is applicable to a much wider range of problems beyond CMB interferometry.

arXiv:1511.03635v4 [astro-ph.CO] 22 Jan 2016

I. INTRODUCTION

Observations of the cosmic microwave background (CMB) are among the chief drivers of the revolutionary advances in cosmology over the past 20 years (see, *e.g.*, [1, 2] and references therein), and further observations, particularly of CMB polarization, are likely to be of major importance in the coming years. CMB polarization can probe the early Universe in a wide variety of ways, including possibly providing direct evidence of a stochastic gravitational wave background, which would give direct evidence in support of inflation [3–6].

The key to analyzing CMB polarization data is the separation of the signal into a scalar E component and a pseudoscalar B component. The inflationary signal is sought in the B component. Because this component is predicted to be significantly weaker than the E component (and both are much weaker than the temperature anisotropy), detection of B modes is a daunting task.

Control of systematic errors will be vital to the success of the quest to characterize B modes. In particular, some errors may cause "leakage" into the B signal from the much larger E and temperature anisotropy (T) signals. (Such leakage occurs even in the absence of systematic errors. See, *e.g.*, [7–20].) In considering the design of future instruments, methods of assessing the severity of various sources of error are quite valuable. Detailed simulations (*e.g.*, [21–24]) often provide the best assessment, but approximate analytic methods (*e.g.*, [25, 26]) can provide valuable insight before undertaking the computational effort of a full simulation.

In this paper, we describe a Fisher-matrix method for assessing the ability of interferometric instruments to detect CMB polarization signals, with particular emphasis on the effect of systematic errors. Interferometers have been important in CMB science in the past, including making some of the early detections of CMB polarization [27, 28]. The formalism for analyzing interferometric CMB observations has been well-developed [29–34] Although most current and planned instruments are traditional imaging telescopes, at least one interferometer is under development [35, 36]. Interferometers and imaging telescopes have quite different susceptibility to various sources of error, so it would seem worthwhile to develop tools to understand both approaches.

The method described in this paper uses Fisher matrices to forecast the errors on cosmological parameters obtainable from a given instrument. After developing the general method for calculating Fisher matrices and the resulting error forecasts for an ideal (systematic-error-free) interferometer, we extend the method to allow consideration of systematic effects. In particular, we calculate an "augmented Fisher matrix," in which we treat parameters describing the various systematic effects as unknowns to be estimated along with the cosmological parameters of interest. The resulting Fisher matrices allow us to forecast the errors expected on cosmological parameters, taking into account our ignorance of the systematic error parameters.

Although we apply our formalism to the specific case of CMB polarization measurements, the approach we describe has broader applicability. In particular, upcoming efforts to map the Universe through 21-cm tomography (see, *e.g.*, [37, 38] and references therein) involve the extraction of faint signals from interferometric data sets and hence have significant overlap with CMB polarization. It would be of interest to explore the generalization of our approach to this class of observations.

The remainder of this paper is organized as follows. Section II lays out the formalism for calculating covariance matrices and Fisher matrices for interferometers, including systematic effects. Section III reviews the approximate analytic treatment of systematic effects in ref. [26]. Section IV presents the results of a variety of tests of the method, and Section V provides a brief discussion.

II. FORMALISM

A. Visibilities

Consider a close-packed square array with N_a antennas on each side. For antennas j and k that are separated by

*Electronic address: haonan.liu@richmond.edu

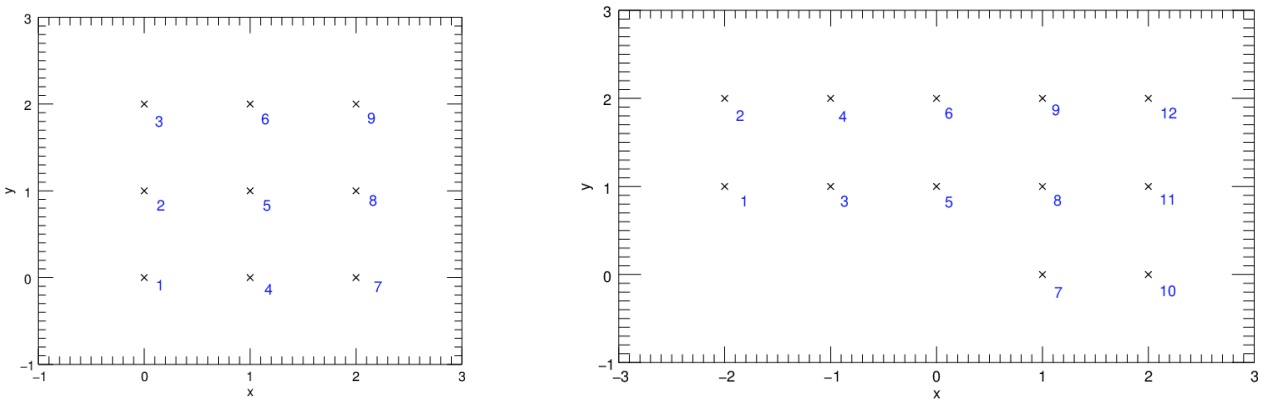

FIG. 1: A close-packed square array and its corresponding baseline graph with $N_a = 3$.

the vector $\delta\mathbf{r} = (x, y)$ on the antenna map, the baseline $\mathbf{u}$ has the form

$$\mathbf{u} = \delta\mathbf{r}\Delta u = (x\Delta u, y\Delta u). \tag{2.1}$$

Here x and y are any integers that satisfy $-(N_a - 1) \leqslant x, y \leqslant N_a - 1$. The baseline for two adjacent antennas is $\Delta u = D/\lambda$, where D is the antenna diameter. We will assume diffraction-limited antennas, for which the Gaussian beam width is $b = 0.518\lambda/D$, so that $\Delta u = 0.518/b$.

The total number of independent baselines is $\frac{1}{2}[(2N_a - 1)^2 - 1]$, where the -1 appears because we do not include the case $x = y = 0$, and the $\frac{1}{2}$ is included to avoid redundancy since $V(\mathbf{u}) = V^*(-\mathbf{u})$. We include all baselines with $y > 0$ and all with $y = 0$ and $x \geq 0$, labeling them in the order shown in Figure 1.

Now, suppose a monochromatic plane wave with angular frequency $\omega = 2\pi c/\lambda$ that approaches the center of one antenna from the direction $\hat{\mathbf{r}}$ has the form

$$\mathbf{E} = \boldsymbol{\epsilon}(\hat{\mathbf{r}})e^{i(\omega t - \mathbf{k}\cdot\mathbf{x})}, \tag{2.2}$$

where $\mathbf{k}$ is the wavevector defined by $\mathbf{k} = -(2\pi/\lambda)\hat{r}$. Then the 2×2 matrix of visibilities corresponding to a given baseline $\mathbf{u}$ is [26]

$$\mathbf{V}(\mathbf{u}) = \int \mathbf{S}(\mathbf{r})A(\mathbf{r})e^{2\pi i\mathbf{u}\cdot\mathbf{r}}d^2\mathbf{r}, \tag{2.3}$$

where the Stokes matrix $\mathbf{S}$ is given by

$$\begin{aligned}\mathbf{S} &= \begin{pmatrix} S_{XX} & S_{XY} \\ S_{YX} & S_{YY} \end{pmatrix} \\ &= \begin{pmatrix} I + Q & U + iV \\ U - iV & I - Q \end{pmatrix},\end{aligned} \tag{2.4}$$

and $A(\mathbf{r})$ is the antenna pattern, which we will take to be Gaussian,

$$A(\mathbf{r}) = e^{-\mathbf{r}^2/2b^2} \tag{2.5}$$

with b the beam size. Note that we are considering experiments that combine linear polarization states (X, Y), not circular polarization states.

We define Stokes Q and U visibilities,

$$V_Q \equiv V_Q(\mathbf{u}) = \int Q(\mathbf{r})A(\mathbf{r})e^{2\pi i\mathbf{u}\cdot\mathbf{r}}d^2\mathbf{r}, \tag{2.6}$$

$$V_U \equiv V_U(\mathbf{u}) = \int U(\mathbf{r})A(\mathbf{r})e^{2\pi i\mathbf{u}\cdot\mathbf{r}}d^2\mathbf{r}. \tag{2.7}$$

As usual in CMB studies, we will express Stokes parameters and their associated visibilities in thermodynamic temperature units.

By the convolution theorem,

$$V_Q = (2\pi)^2 \int\int \tilde{Q}(\mathbf{k})\tilde{A}^*(\mathbf{k} + 2\pi\mathbf{u})d^2\mathbf{k}, \tag{2.8}$$

$$V_U = (2\pi)^2 \int\int \tilde{U}(\mathbf{k})\tilde{A}^*(\mathbf{k} + 2\pi\mathbf{u})d^2\mathbf{k}, \tag{2.9}$$

where the tilde denotes a two-dimensional Fourier transform in the flat-sky approximation.

From equation (2.4), we can see that the Q and U visibilities are related to the visibility matrix $\mathbf{V}$ by

$$V_Q = \frac{1}{2}(V_{XX} - V_{YY}), \tag{2.10}$$

$$V_U = \frac{1}{2}(V_{XY} + V_{YX}). \tag{2.11}$$

In practice, we do not usually use (2.10) to measure V_Q, as it involves cancellation of the large contribution from Stokes I. Instead, we usually measure V_Q by rotating the axes for our polarization basis through 45° and then using equation (2.11).

The Stokes parameters are related to the E and B modes in the following way:

$$\tilde{Q}(\mathbf{k}) = \tilde{E}(\mathbf{k})\cos(2\phi) + \tilde{B}(\mathbf{k})\sin(2\phi), \tag{2.12}$$

$$\tilde{U}(\mathbf{k}) = -\tilde{E}(\mathbf{k})\sin(2\phi) + \tilde{B}(\mathbf{k})\cos(2\phi), \tag{2.13}$$

where ϕ is the angle between the vector $\mathbf{k}$ and the x axis. We assume that the E and B contributions are independent, statistically isotropic random fields with the flat-sky power spectra P_E, P_B, which are defined as $P_{E,B}(k) = C_l^{E,B}$ with $l = k$. Then

$$\langle \tilde{E}(\mathbf{k}_1)\tilde{E}^*(\mathbf{k}_2)\rangle = \frac{P_E(k_1)}{(2\pi)^2}\delta(\mathbf{k}_1 - \mathbf{k}_2), \tag{2.14}$$

with a similar expression for B. The extra $(2\pi)^2$ factor is caused by the approximation of a flat-sky power spectrum from a full sky power spectrum.

We then have

$$\langle \tilde{Q}(\mathbf{k}_1)\tilde{Q}^*(\mathbf{k}_2)\rangle = \delta(\mathbf{k}_1 - \mathbf{k}_2)/(2\pi)^2 [P_E(\mathbf{k})\cos^2(2\phi) + P_B(\mathbf{k})\sin^2(2\phi)], \tag{2.15}$$

$$\langle \tilde{U}(\mathbf{k}_1)\tilde{U}^*(\mathbf{k}_2)\rangle = \delta(\mathbf{k}_1 - \mathbf{k}_2)/(2\pi)^2 [P_E(\mathbf{k})\sin^2(2\phi) + P_B(\mathbf{k})\cos^2(2\phi)], \tag{2.16}$$

$$\langle \tilde{Q}(\mathbf{k}_1)\tilde{U}^*(\mathbf{k}_2)\rangle = \delta(\mathbf{k}_1 - \mathbf{k}_2)/(2\pi)^2 [-\frac{1}{2}P_E(\mathbf{k})\sin(4\phi) + \frac{1}{2}P_B(\mathbf{k})\sin^2(2\phi)]. \tag{2.17}$$

We will use these results in the next section for the deduction of the visibility covariance matrix.

For regular arrays of the sort considered here, multiple pairs of antennas can have the same separation vector $\delta\mathbf{r}$ and hence correspond to the same baseline. We refer to the visibility measured from a given antenna pair as a "micro-visibility" and say that multiple micro-visibilities correspond to the same "macro-visibility." Since all micro-visibilities corresponding to a given macro-visibility should be equal (in the absence of noise), we average them together to get the measured value of the macro-visibility.

To be specific, let V_J represent the Jth macro-visibility. Let S_J be the set of all micro-visibilities corresponding to that macro-visibility, with each micro-visibility labeled by a pair of antennas (ab). Also let N_J be the number of micro-visibilities corresponding to that macro-visibility (i.e., the cardinality of S_J). Then

$$V_{XJ} = \frac{1}{N_J}\sum_{(ab)\in S_J} V_X^{(ab)}, \tag{2.18}$$

where $X \in \{Q, U\}$, and $V_X^{(ab)}$ labels a micro-visibility.

For instance, consider a 3×3 array with antennas labeled from 1 to 9 as in Figure 1. There are twelve macro-visibilities. Using the numbering scheme in the figure, $J = 7$ corresponds to the macro-visibility $(1, 0)$ – that is, to antennas that are separated by one unit in the x direction and zero units in the y direction. Then

$$S_7 = \{(14), (25), (36), (47), (58), (69)\}, \tag{2.19}$$

and of course $N_7 = 6$.

B. Fisher Information Matrix

1. Real Values

Although we will be working with complex data (visibilities), we begin by reviewing the Fisher matrix formalism for real data.

Let $\vec{r} = (r_1, \ldots, r_n)^T$ be a random vector drawn from a multivariate normal distribution with mean zero and covariance matrix $\mathbf{\Gamma}$ with elements

$$\Gamma_{jk} = \langle r_i r_j\rangle. \tag{2.20}$$

The probability density for $\vec{r}$ is

$$f(\vec{r}) = \frac{e^{-\frac{1}{2}\vec{r}^T\mathbf{\Gamma}^{-1}\vec{r}}}{(2\pi)^{n/2}\det^{1/2}(\mathbf{\Gamma})}. \tag{2.21}$$

Now suppose that $\mathbf{\Gamma}$ is a function of some set of m parameters $\theta_1, \theta_2, \ldots, \theta_m$. These may be cosmological parameters which we would like to estimate from the data, but as we will see they can also be parameters characterizing the experiment itself (e.g., the gain on an antenna or the orientation of a polarizer).

We define the likelihood function

$$L(\vec{\theta}) = f(\vec{r}|\vec{\theta}). \tag{2.22}$$

For convenience, define the log-likelihood function

$$\mathcal{L} = -\ln L = \frac{1}{2}\vec{r}^T\mathbf{\Gamma}^{-1}\vec{r} + \frac{1}{2}\ln\det(\mathbf{\Gamma}) + \frac{n}{2}\ln(2\pi). \tag{2.23}$$

Then the Fisher Information Matrix is defined to have elements

$$F_{jk} = \left\langle \frac{\partial^2\mathcal{L}}{\partial\theta_j\partial\theta_k}\right\rangle, \tag{2.24}$$

which can be shown to be

$$F_{jk} = \frac{1}{2}\mathrm{Tr}\left(\mathbf{\Gamma}^{-1}\frac{d\mathbf{\Gamma}}{d\theta_j}\mathbf{\Gamma}^{-1}\frac{d\mathbf{\Gamma}}{d\theta_k}\right). \tag{2.25}$$

The Fisher matrix tells us the expected errors on the parameters. In particular, $1/\sqrt{F_{ii}}$ is the expected error on θ_i assuming all the other parameters are known, and $\sqrt{(F^{-1})_{ii}}$ is the optimal error on θ_i assuming all other parameters are unknown (*e.g*, [39]).

2. Complex Values

We now consider complex vectors. Let $\vec{z} = (z_1, \ldots, z_n)^T$ be a vector of complex Gaussian random numbers with zero mean (e.g., a set of visibilities). One way to proceed is to think of this n-dimensional complex

vector as a $2n$-dimensional real vector. To be specific, let $\vec{x} = \mathrm{Re}(\vec{z})$ and $\vec{y} = \mathrm{Im}(\vec{z})$, and define

$$\vec{r} = \begin{pmatrix} \vec{x} \\ \vec{y} \end{pmatrix} = \begin{pmatrix} x_1 \\ \vdots \\ x_n \\ y_1 \\ \vdots \\ y_n \end{pmatrix}. \tag{2.26}$$

Then define a $2n \times 2n$ covariance matrix

$$\mathbf{\Gamma}^{(r)} = \begin{pmatrix} \mathbf{\Gamma}_{xx} & \mathbf{\Gamma}_{xy} \\ \mathbf{\Gamma}_{yx} & \mathbf{\Gamma}_{yy} \end{pmatrix}, \tag{2.27}$$

where the four $n \times n$ sub-matrices are $\mathbf{\Gamma}_{xx} = \langle \vec{x}\vec{x}^T \rangle$, etc. Then all of the results of the previous section apply.

Often, it is inconvenient to express complex vectors in terms of the real and imaginary parts as above. Instead, we define two new matrices: the complex covariance matrix $\mathbf{\Gamma}$ and the complex relation matrix $\mathbf{C}$ with elements

$$\Gamma_{jk} = \langle z_j z_k^* \rangle, \tag{2.28}$$

$$C_{jk} = \langle z_j z_k \rangle. \tag{2.29}$$

It is straightforward to check that

$$\mathbf{\Gamma} = \mathbf{\Gamma}_{xx} + \mathbf{\Gamma}_{yy} + i(\mathbf{\Gamma}_{yx} - \mathbf{\Gamma}_{xy}) \tag{2.30}$$

$$\mathbf{C} = \mathbf{\Gamma}_{xx} - \mathbf{\Gamma}_{yy} + i(\mathbf{\Gamma}_{yx} + \mathbf{\Gamma}_{xy}). \tag{2.31}$$

These two methods of approaching the complex Gaussian vectors are closely related. To see this relationship, define another $2n$-dimensional vector

$$\vec{c} = \begin{pmatrix} \vec{z} \\ \vec{z}^* \end{pmatrix}. \tag{2.32}$$

Then

$$\vec{c} = \mathbf{B}\vec{r}, \tag{2.33}$$

where $\mathbf{B}$ can be written in block form as

$$\mathbf{B} = \begin{pmatrix} \mathbf{I} & i\mathbf{I} \\ \mathbf{I} & -i\mathbf{I} \end{pmatrix}, \tag{2.34}$$

and $\mathbf{I}$ is the n-dimensional identity matrix. Then

$$\mathbf{\Gamma}^{(c)} \equiv \langle \vec{c}\vec{c}^\dagger \rangle = \begin{pmatrix} \langle \vec{z}\vec{z}^\dagger \rangle & \langle \vec{z}\vec{z}^T \rangle \\ \langle \vec{z}\vec{z}^T \rangle^* & \langle \vec{z}\vec{z}^\dagger \rangle^* \end{pmatrix} = \begin{pmatrix} \mathbf{\Gamma} & \mathbf{C} \\ \mathbf{C}^* & \mathbf{\Gamma}^* \end{pmatrix}. \tag{2.35}$$

But we can also write

$$\mathbf{\Gamma}^{(c)} = \langle \vec{c}\vec{c}^\dagger \rangle = \mathbf{B}\langle \vec{r}\vec{r}^T \rangle \mathbf{B}^\dagger. \tag{2.36}$$

Setting these two expressions equal gives us

$$\mathbf{\Gamma}^{(c)} = \mathbf{B}\mathbf{\Gamma}^{(r)}\mathbf{B}^\dagger, \tag{2.37}$$

$$\mathbf{\Gamma}^{(r)} = \mathbf{B}^{-1}\mathbf{\Gamma}^{(c)}(\mathbf{B}^\dagger)^{-1} = \frac{1}{4}\mathbf{B}^\dagger\mathbf{\Gamma}^{(c)}\mathbf{B}, \tag{2.38}$$

using the fact that $\mathbf{B}^{-1} = \frac{1}{2}\mathbf{B}^\dagger$. Equations (2.37) and (2.38) provide a convenient way of converting back and forth between the real $(\vec{x}, \vec{y})$ and complex $(\vec{z}, \vec{z}^*)$ representations of our random vector.

Equation (2.21) gives the probability density for a $2n$-dimensional real vector:

$$f(\vec{r}) = \frac{e^{-\frac{1}{2}\vec{r}^T(\mathbf{\Gamma}^{(r)})^{-1}\vec{r}}}{(2\pi)^n \det^{1/2}(\mathbf{\Gamma}^{(r)})}. \tag{2.39}$$

We can write this in terms of the complex vector $\vec{c}$ using $\vec{r} = \mathbf{B}^{-1}\vec{c}$:

$$f(\vec{c}) = \frac{e^{-\frac{1}{2}\vec{c}^\dagger(\mathbf{\Gamma}^{(c)})^{-1}\vec{c}}}{\pi^n \det^{1/2}(\mathbf{\Gamma}^{(c)})}. \tag{2.40}$$

The factor 2 in equation (2.39) is missing in equation (2.40) because $\det(\mathbf{\Gamma}^{(c)}) = |\det(\mathbf{B})|^2 \det(\mathbf{\Gamma}^{(r)})$, and $\det(\mathbf{B}) = (-2i)^n$.

The Fisher matrix elements are given by equation (2.25), using $\mathbf{\Gamma}^{(r)}$ as the covariance matrix. If, as is often the case, it is easier to work with $\mathbf{\Gamma}^{(c)}$, we simply use equation (2.38) to relate the two matrices. We will apply these results to the vector of complex visibilities in the next section.

C. Visibility Covariance Matrix and Fisher Matrix

We now apply the results of the previous section to visibility data. Suppose that our data consists of a set of visibilities $\vec{c} = (V_Q(\mathbf{u}_1), V_Q(\mathbf{u_2}), \ldots, V_U(\mathbf{u}_1), V_U(\mathbf{u}_2), \ldots)$. Consider an element of the upper left quadrant of the covariance matrix $\mathbf{\Gamma}$, which is the covariance of two Q visibilities. According to equations (2.8) and (2.15),

$$\begin{aligned} &\langle V_Q(\mathbf{u}_1) V_Q^*(\mathbf{u}_2) \rangle \\ &= (2\pi)^2 \int \langle \tilde{Q}(\mathbf{k}_1)\tilde{Q}^*(\mathbf{k}_2) \rangle \tilde{A}^*(\mathbf{k}_1 + 2\pi\mathbf{u}_1)\tilde{A}(\mathbf{k}_2 + 2\pi\mathbf{u}_2) d^2\mathbf{k} \\ &= (2\pi)^2 \int (\delta(\mathbf{k}_1 - \mathbf{k}_2)[P_E(\mathbf{k})\cos^2(2\phi) + P_B(\mathbf{k})\sin^2(2\phi)] \\ &\quad \tilde{A}^*(\mathbf{k}_1 + 2\pi\mathbf{u}_1)\tilde{A}(\mathbf{k}_2 + 2\pi\mathbf{u}_2) d^2\mathbf{k} \\ &= (2\pi)^2 \int [P_E(\mathbf{k})\cos^2(2\phi) + P_B(\mathbf{k})\sin^2(2\phi)] \\ &\quad \tilde{A}^*(\mathbf{k} + 2\pi\mathbf{u}_1)\tilde{A}(\mathbf{k} + 2\pi\mathbf{u}_2) d^2\mathbf{k}. \end{aligned} \tag{2.41}$$

As long as A is isotropic, this expression and the corresponding ones for $\langle V_Q V_U^* \rangle$ and $\langle V_U V_U^* \rangle$ can be expressed as a single integral by writing d^2k in polar coordinates and integrating over the angular coordinate, as shown in the Appendix.

As long as the antenna pattern A has reflection symmetry, $\tilde{A}$ is real, and hence $\langle V_Q(\mathbf{u}_1) V_Q^*(\mathbf{u}_2) \rangle$ is real as well. By similar reasoning, $\langle V_Q(\mathbf{u}_1) V_U^*(\mathbf{u}_2) \rangle$ and $\langle V_U(\mathbf{u}_1) V_U^*(\mathbf{u}_2) \rangle$ are also real. Hence we conclude $\mathbf{\Gamma}$ is real for visibility data. The same is true for the relation matrix $\mathbf{C}$.

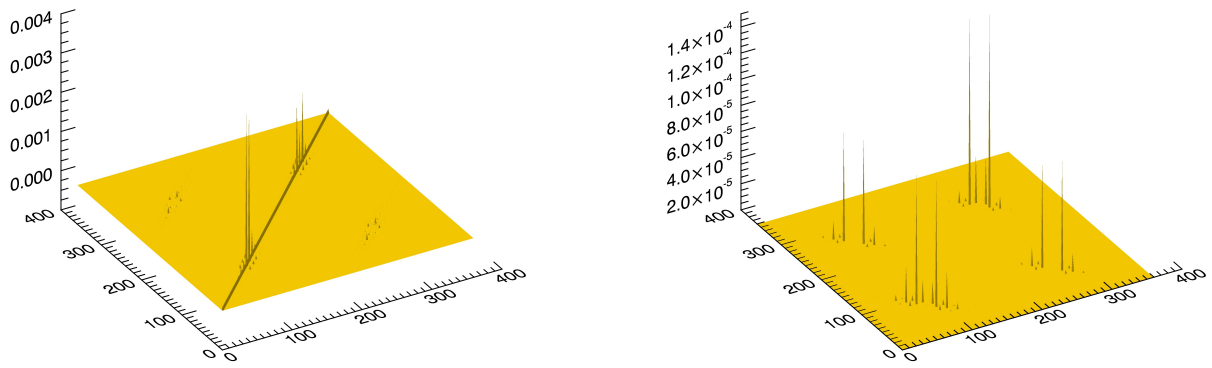

FIG. 2: Covariance and relation matrices $\mathbf{\Gamma}$ and $\mathbf{C}$ for an array with $N_a = 10$, $b = 0.0873$ rad, noise $n = 0.01\,\mu$K. The sizes of both matrices are 360×360 and the unit of the vertical axis is μK^2. Notice that noise only affects the $\mathbf{\Gamma}$ matrix.

Since $\mathbf{\Gamma}_{xx}$, $\mathbf{\Gamma}_{yy}$, $\mathbf{\Gamma}_{yx}$ and $\mathbf{\Gamma}_{xy}$ are all real, equations (2.30) and (2.31) imply that $\mathbf{\Gamma}_{yx} - \mathbf{\Gamma}_{xy} = \mathbf{\Gamma}_{yx} + \mathbf{\Gamma}_{xy} = 0$, and hence that

$$\mathbf{\Gamma}_{yx} = \mathbf{\Gamma}_{xy} = 0, \tag{2.42}$$
$$\mathbf{\Gamma}_{xx} = (\mathbf{\Gamma} + \mathbf{C})/2, \tag{2.43}$$
$$\mathbf{\Gamma}_{yy} = (\mathbf{\Gamma} - \mathbf{C})/2. \tag{2.44}$$

Therefore, from the definition of $\mathbf{\Gamma}^{(r)}$ (2.27), we see that $\mathbf{\Gamma}^{(r)}$ is a block matrix

$$\mathbf{\Gamma}^{(r)} = \begin{pmatrix} \mathbf{\Gamma}_{xx} & 0 \\ 0 & \mathbf{\Gamma}_{yy} \end{pmatrix} = \begin{pmatrix} (\mathbf{\Gamma} + \mathbf{C})/2 & 0 \\ 0 & (\mathbf{\Gamma} - \mathbf{C})/2 \end{pmatrix}. \tag{2.45}$$

An example of $\mathbf{\Gamma}$ and $\mathbf{C}$ can be found in Figure 2.

Now we attain the final form for the visibility Fisher matrix

$$F_{jk} = \frac{1}{2}\text{Tr}\left((\mathbf{\Gamma}_{xx})^{-1} \frac{d\mathbf{\Gamma}_{xx}}{d\theta_j} (\mathbf{\Gamma}_{xx})^{-1} \frac{d\mathbf{\Gamma}_{xx}}{d\theta_k} \right) + \frac{1}{2}\text{Tr}\left((\mathbf{\Gamma}_{yy})^{-1} \frac{d\mathbf{\Gamma}_{yy}}{d\theta_j} (\mathbf{\Gamma}_{yy})^{-1} \frac{d\mathbf{\Gamma}_{yy}}{d\theta_k} \right) \tag{2.46}$$

D. The Augmented Fisher Matrix

The Fisher matrix allows us to compute the expected errors on cosmological parameters for an ideal experiment. We now want to introduce the possibility of sources of systematic error. Suppose that there is some imperfectly-known aspect of the experimental setup that can be characterized by a parameter p. The experimenter has measured p with some uncertainty, so that the probability density is sharply peaked around some measured value $\hat{p}$. Often, we are willing to assume that the probability density $f(p|\hat{p})$ is Gaussian with mean $\hat{p}$ and known variance σ_p^2.

Let us include the experimental parameter p along with the cosmological parameters $\vec{\theta}$ in the likelihood function:

$$L(\vec{\theta}, p) \equiv f(\vec{r}, p|\vec{\theta}, \hat{p}) = f(\vec{r}|\vec{\theta}, p) f(p|\hat{p}) = \left(\frac{\exp\left(-\frac{1}{2}\vec{r}^T \mathbf{\Gamma}^{-1} \vec{r}\right)}{(2\pi)^{n/2} \det{}^{1/2}(\mathbf{\Gamma})} \right) \left(\frac{\exp(-(p-\hat{p})^2/2\sigma_p^2)}{\sqrt{2\pi}\,\sigma_p} \right). \tag{2.47}$$

In this expression, the covariance matrix $\mathbf{\Gamma}$ depends on both the cosmological parameters $\vec{\theta}$ and the experimental parameter p.

We want to determine the effect that our ignorance of p has on our attempt to measure $\vec{\theta}$. We can do this by treating p along with $\vec{\theta}$ as unknowns to be estimated simultaneously and calculating an "augmented" Fisher matrix whose rows and columns correspond to the parameters $\vec{\theta}^{(a)} = (\theta_1, \theta_2, \ldots, \theta_m, p)$.

The log-likelihood is given by

$$\mathcal{L} \equiv -\ln L = \frac{1}{2}\left(\vec{r}^T \mathbf{\Gamma}^{-1} \vec{r} + \ln\det\mathbf{\Gamma} + \frac{(p-\hat{p})^2}{\sigma_p^2} \right) + \text{const.} \tag{2.48}$$

In calculating the Fisher matrix elements $F_{jk} = -\langle \partial^2 \mathcal{L} / \partial\theta_j^{(a)} \partial\theta_k^{(a)} \rangle$, the ensemble average in principle includes an average over all possible values of $\hat{p}$ as well as over all possible values of $\vec{r}$. However, it happens that all second derivatives of $\mathcal{L}$ with respect to $\vec{\theta}$ and p are independent of $\hat{p}$, so the averaging over $\hat{p}$ has no effect. Thus, the upper left $m \times m$ block of the augmented Fisher matrix is still given by equation (2.46). All that remains is to determine the final row and column.

For $j \le m$ we have

$$F_{j,m+1} = \frac{1}{2}\mathrm{Tr}\left((\mathbf{\Gamma}^{(r)})^{-1}\frac{\partial \mathbf{\Gamma}^{(r)}}{\partial \theta_j}(\mathbf{\Gamma}^{(r)})^{-1}\frac{\partial \mathbf{\Gamma}^{(r)}}{\partial p}\right). \quad (2.49)$$

Note that this is just the usual Fisher matrix element, treating p as a normal cosmological parameter. The very last term, in the lower right corner has an extra $1/\sigma_p^2$ in it

$$F_{m+1,m+1} = \frac{1}{2}\mathrm{Tr}\left((\mathbf{\Gamma}^{(r)})^{-1}\frac{\partial \mathbf{\Gamma}^{(r)}}{\partial p}(\mathbf{\Gamma}^{(r)})^{-1}\frac{\partial \mathbf{\Gamma}^{(r)}}{\partial p}\right) + \frac{1}{\sigma_p^2}, \quad (2.50)$$

arising from the term $(p-\hat{p})^2/\sigma_p^2$ in equation (2.48).

In the formulae above we have assumed that we only have one systematic parameter. The generalization to n parameters is straightforward, leading to an $(m+n)\times(m+n)$ augmented Fisher matrix.

E. Rotation errors

In section IV, we consider two examples of systematic errors: gain errors and rotation errors. In order to assess the effect of these errors on power spectrum estimates, we need to know their effects on the visibility covariance matrix. The case of gain errors is trivial: a gain error g on a given antenna multiplies all of the micro-visibilities involving that antenna by $1+g$. The case of rotation errors requires more attention.

Suppose that each antenna j has its polarizers rotated by some unknown angle p_j, with corresponding rotation matrix $\mathbf{R}_j = \mathbf{R}(p_j)$. Consider a measurement of a micro-visibility pair $(V_{Q,(ab)}, V_{U,(ab)})$, where (ab) labels an atenna pair. Then the observed Stokes matrix $\mathbf{S}$ of (2.4) is related to the true (error-free) matrix $\hat{\mathbf{S}}$ as

$$\mathbf{S} = \mathbf{R}_a\hat{\mathbf{S}}\mathbf{R}_b^\dagger. \quad (2.51)$$

Because the visibilities are linearly related to the matrix $\mathbf{S}$, they obey a similar rule:

$$\mathbf{V} = \mathbf{R}_a\hat{\mathbf{V}}\mathbf{R}_b^\dagger \quad (2.52)$$

Applying the rotation matrices to the Stokes visibility matrix, we find that

$$V_{Q(ab)} = \hat{V}_{Q(ab)}\cos(p_a+p_b) + \hat{V}_{U(ab)}\sin(p_a+p_b), \quad (2.53)$$

$$V_{U(ab)} = -\hat{V}_{Q(ab)}\sin(p_a+p_b) + \hat{V}_{U(ab)}\cos(p_a+p_b). \quad (2.54)$$

That is, the visibilities $\begin{pmatrix} V_{Q(ab)} \\ V_{U(ab)}\end{pmatrix}$ are simply multiplied by the rotation matrix corresponding to (p_a+p_b).

Now consider the covariance between two pairs of *macro*-visibilities V_{XJ} and V_{XK}, where $X \in \{Q,U\}$ and J,K label the visibilities. We can express their covariances as a 2×2 submatrix of the full covariance matrix:

$$\mathbf{C} = \left\langle \mathbf{v}_J\mathbf{v}_K^\dagger \right\rangle, \quad (2.55)$$

where

$$\mathbf{v}_J = \begin{pmatrix} V_{QJ} \\ V_{UJ}\end{pmatrix}. \quad (2.56)$$

In the absence of systematic errors, the covariance matrix is

$$\mathbf{C_0} = \frac{1}{N_J N_K}\sum_{(ab)\in S_J}\sum_{(cd)\in S_K}\left\langle \mathbf{v}_{(ab)}\mathbf{v}_{(cd)}^\dagger\right\rangle \quad (2.57)$$

As we saw above, each micro-visibility is modified as follows:

$$\mathbf{v}_{(ab)} \to \mathbf{R}_a\mathbf{R}_b\mathbf{v}_{(ab)}. \quad (2.58)$$

The 2×2 covariance matrix corresponding to macro-visibilities J,K is therefore

$$\begin{aligned}\mathbf{C} &= \frac{1}{N_J N_K}\sum_{(ab)\in S_J}\sum_{(cd)\in S_K}\left\langle \mathbf{v}_{(ab)}\mathbf{v}_{(cd)}^\dagger\right\rangle \\ &= \frac{1}{N_J N_K}\sum_{(ab)\in S_J}\sum_{(cd)\in S_K}\mathbf{R}_a\mathbf{R}_b\mathbf{C}_0\mathbf{R}_d^\dagger\mathbf{R}_c^\dagger \\ &= \left(\frac{1}{N_J}\sum_{(ab)\in S_J}\mathbf{R}_a\mathbf{R}_b\right)\mathbf{C}_0\left(\frac{1}{N_K}\sum_{(cd)\in S_K}\mathbf{R}_c\mathbf{R}_d\right)^\dagger \\ &= \mathcal{R}_J\mathbf{C}_0\mathcal{R}_K^\dagger, \end{aligned} \quad (2.59)$$

where the matrices $\mathcal{R}$ are defined by the last line.

We can apply this rule to each pair of macro-visibilities to determine the effect of the rotation errors on the entire visibility covariance matrix.

III. APPROXIMATE ANALYTIC TREATMENT

Bunn [26] gave an approximate analytic treatment of various sources of systematic errors in CMB interferometry. We will compare the full Fisher matrix calculation described above to this treatment. In this section, we briefly review and extend the methods outlined in that paper.

A. Statistical errors on power spectrum estimates

Before introducing systematic errors, we present a simple method for estimating purely statistical errors on power spectrum estimates.

Following [26], we begin by imagining an experiment that measures only a single visiblity pair (V_Q, V_U). According to equation (4.8b) of [26], for a single visibility

pair, we can find an unbiased estimator of C_l^B in a band centered on $l = 2\pi u$,

$$\hat{C}_{B,\rm single} = (\pi b^2)^{-1}\gamma(\overline{c^2}|V_U|^2 - \overline{s^2}|V_Q|^2), \tag{3.1}$$

where b is the beam size,

$$\gamma = [(\overline{c^2})^2 - (\overline{s^2})^2]^{-1}, \tag{3.2}$$

and

$$\overline{c^2} = \frac{\int |\tilde{A}^2(\mathbf{k}+2\pi\mathbf{u})|^2\cos^2(\phi)d^2\mathbf{k}}{\int |\tilde{A}^2(\mathbf{k}+2\pi\mathbf{u})|^2 d^2\mathbf{k}} \tag{3.3}$$

$$\overline{s^2} = \frac{\int |\tilde{A}^2(\mathbf{k}+2\pi\mathbf{u})|^2\sin^2(\phi)d^2\mathbf{k}}{\int |\tilde{A}^2(\mathbf{k}+2\pi\mathbf{u})|^2 d^2\mathbf{k}} = 1 - \overline{c^2} \tag{3.4}$$

We have defined θ_B as the ratio of measured to true power, so the estimator of this quantity is $\hat{\theta}_{B,\rm single} = \hat{C}_B/C_B$. After some algebra, we find that the variance of $\theta_{B,\rm single}$ is

$$\begin{aligned}\sigma^2_{B,\rm single} &= \langle\hat{\theta}^2_{B,\rm single}\rangle - \langle\hat{\theta}_{B,\rm single}\rangle^2 \\ &= \gamma^2\left[2(\overline{c^2})^2(\overline{s^2})^2\left(\frac{C_E}{C_B}\right)^2 + ((\overline{c^2})^4 + (\overline{s^2})^4)\right. \\ &\left. +(2(\overline{c^2})^3\overline{s^2} + 2(\overline{s^2})^3\overline{c^2})\left(\frac{C_E}{C_B}\right)\right]\end{aligned} \tag{3.5}$$

We now consider an experiment with many measured macro-visibilities, and regard each macro-visibility pair as an independent measurement of θ_B. Then the minimum-variance estimator from the entire data set is the usual weighted average, with weights given by the inverse variance, and the variance of this estimator is

$$\sigma^2_{B,\rm final} = \left(\sum_J \sigma_{BJ}^{-2}\right)^{-1}, \tag{3.6}$$

where σ^2_{BJ} is given by (3.5) for baseline J.

In Section IV, we will compare the results of this simple approximation with the full Fisher matrix calculation, as well as with the approximation in which calculate the fisher matrix while keeping only diagonal elements of the (real) covariance matrix.

B. Systematic errors

We now summarize the key results of [26]. Once again, we begin by imagining measurements of the intensity and polarization visibilities, $\mathbf{v} \equiv (V_I, V_Q, V_U)^T$ for a single baseline. In many cases, the leading-order effect of a systematic error is to "mix" the visibilities, inducing errors $\delta\mathbf{v} = \mathbf{E}\cdot\mathbf{v}$ for some mixing matrix $\mathbf{E}$.

If the experimenter then uses the data set $\mathbf{v}$ to optimally estimate the E and B power spectra, without accounting for the effect of the systematic error, then the resulting estimates will have errors given by

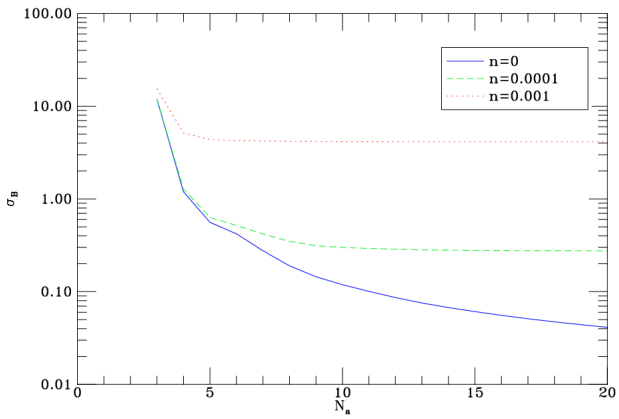

FIG. 3: The relation between σ_B and N_a for noise levels 0, $0.0001\,\mu$K, and $0.001\,\mu$K. The beam size $b = 0.0873$ rad.

$$\left(\delta\hat{C}^K_{\rm rms}\right)^2 = p^2\sum_{I,J}\kappa^2_{K,IJ}C^I C^J, \tag{3.7}$$

where $I, J, K \in \{T, X, E, B\}$ label the power spectra (temperature, TE correlation, E polarization, B polarization), p is the rms amplitude of the error under consideration, and the coefficients $\kappa_{K,IJ}$ can be calculated from the error mixing matrix $\mathbf{E}$. Because there is a hierarchy in power spectrum amplitudes, with $T > X > E > B$, one can generally keep only the dominant term in this sum.

For example, for gain errors, the dominant term in the B power spectrum error is the one that corresponds to contamination by E power, with

$$\kappa^2_{B,EE} = 2\gamma^2(\overline{s^2}\,\overline{c^2})^2 \tag{3.8}$$

As in the case of statistical errors above, we can crudely estimate the expected effect of a systematic error in a many-baseline experiment by assuming that each baseline provides an independent power spectrum estimate and performing an appropriate average. See Section V of [26] for details.

Equation (3.6) gives the analytic approximation for σ_B in the absence of systematic errors. In generalizing it to the case where a systematic error is included, we assume that, for each antenna, the error caused by the systematic error p is independent of the statistical error, so that

$$\sigma^2_{Bj} = \sigma^2_{Bj,0} + \sigma^2_{Bj,p}. \tag{3.9}$$

Here σ_{Bj} is the error on the B power spectrum estimate corresponding to the jth micro-visibility. The quantity $\sigma^2_{Bj,0}$ is the noise variance for that visibility in the absence of systematic errors, given by equation (3.5), and $\sigma^2_{Bj,p} = (\delta\hat{C}^B_{\rm rms})^2/C^B_l$ is the additional variance induced

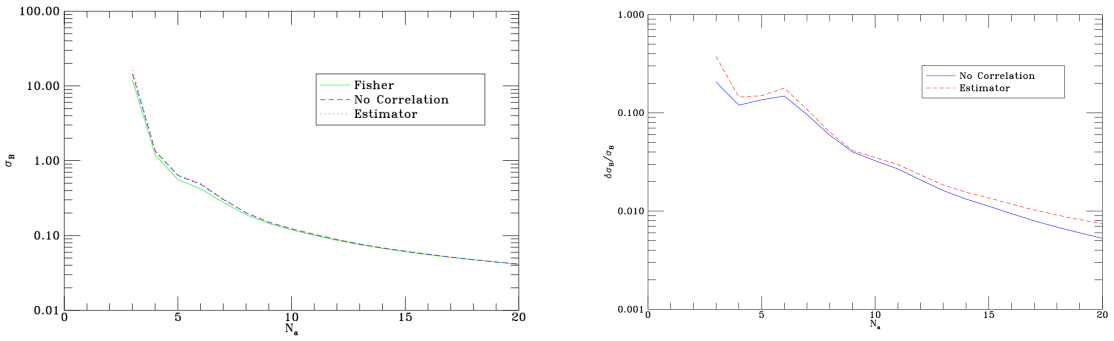

FIG. 4: The relationship between σ_B and N_a in the absence of systematic errors, calculated via the full Fisher matrix, the Fisher matrix with correlations between distinct baselines neglected, and the analytic estimator $\hat{\theta}_B$ of Section III. The left panel shows the errors calculated by the three methods, and the right shows the difference (4.6) between the approximations and the full Fisher calculations. Noise is set to zero in these calculations.

by the systematic error. (Here $l = 2\pi u$ for the given visibility.) Because each macro-visibility is estimated via an average of the corresponding micro-visibilities, we can compute the expected error in our B power spectrum estimate for each macro-visibility. The final error on the B power is then given by equation (3.6).

IV. RESULTS

We have calculated Fisher matrix errors for $N_a \times N_a$ square arrays of close-packed antennas with Gaussian beam width $b = 5^\circ = 0.0873$ rad, as in [22]. We assume that the input power spectra are given by the standard LCDM model [40] with tensor-to-scalar ratio $r = 0.1$, and that the experimenter's goal is to estimate the amplitudes of the E and B power spectra. To be specific, let C^E, C^B be the true power spectra. Then the parameters to be estimated are θ_E, θ_B such that the estimated power spectra are

$$\hat{C}^E = \theta_E C^E \tag{4.1}$$

$$\hat{C}^B = \theta_B C^B \tag{4.2}$$

Since θ_E, θ_B are defined as relative amplitudes, their true value is one. The errors computed for these quantities will therefore be relative errors on the amplitude of the E and B signals. It would be straightforward to generalize these results to the estimation of multiple band powers in E and B.

We are particularly interested in the detectability of the faint B signal. As a result, we will focus on the quantity $\sigma_B = \sqrt{(F^{-1})_{BB}}$, which is the standard deviation of θ_B if none of the other parameters is known.

A. Exact Fisher Matrix with different noise levels

We begin by ignoring all systematic errors and focusing on the effect of noise levels on the Fisher matrix. Assuming that all visibilities are subjected to white noise with standard deviation n, the visibility covariance matrix is

$$\mathbf{\Gamma}_{noise} = \mathbf{\Gamma} + n^2\mathbf{I}, \tag{4.3}$$

where $\mathbf{I}$ is the identity matrix.

Figure 3 shows the relationship between σ_B and N_a for noise levels $n = 0$, 0.0001, and 0.001 μK.[1] For noise-free experiments, σ_B gradually decreases as N_a increases. However, when some noise is present, there is a limit for N_a at which σ_B cannot be attenuated even if we continue to increase the number of antennas.

For further analysis, we set $n = 0.0002\,\mu$K, a value which allows for a detection of B modes but for which noise contributions are still significant.

B. Comparison of calculation methods

In this section, we compare errors calculated using the full Fisher matrix formalism with those based on two approximate methods. One is the analytic approximations described in III. The other is a Fisher-matrix calculation, with the approximation that off-diagonal correlations between visibilities can be neglected – that is, that $\Gamma^{(r)}_{jk} = 0$ for all (j, k) corresponding to macro-visibilities with distinct baselines $\mathbf{u}_j \neq \mathbf{u}_k$.

We begin by considering purely statistical errors and then introduce systematic errors.

[1] If these values seem surprisingly small, note that, with our Fourier transform and antenna pattern normalization conventions, the variance of a visibility is $\sim \pi b^2 C_l^E$.

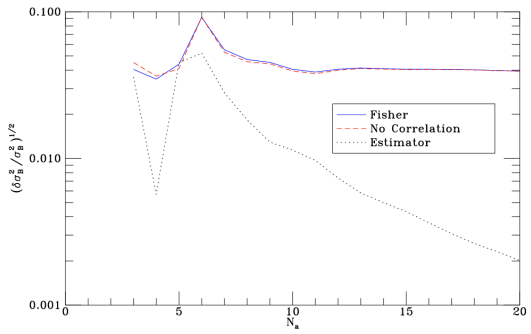

FIG. 5: The effect of a 10% gain error on antenna 6, calculated via the three methods listed in the previous figure. The quantity $\delta\sigma_B^2$ is the difference in variances of the error estimates with and without the gain error. Noise is set to zero in these calculations.

1. *Statistical errors*

We do not consider systematic errors in this section, meaning that our Fisher matrix will only be a 2×2 matrix, corresponding to the two cosmological parameters θ_E, θ_B to be estimated. One example of a typical Fisher matrix is

$$F = \begin{pmatrix} 179 & 4.23 \\ 4.23 & 3.08 \end{pmatrix} \tag{4.4}$$

with inverse

$$F^{-1} = \begin{pmatrix} 0.00577 & -0.00792 \\ -0.00792 & 0.33586797 \end{pmatrix} \tag{4.5}$$

with the parameters $N_a = 10$, beam size $b = 0.0873$ rad, and $n = 0.0002\,\mu$K. (We give extra significant figures for the σ_B term for comparison with later results.) This matrix indicates, for instance, that with the given parameters the least possible variance for measuring θ_B is 0.336, relative to its mean value 1.

Figure 4 compares the values of σ_B calculated via the three methods. In these calculations, $b = 0.0873$ as usual, but the noise level is set to zero. The left panel shows $\sigma_B \equiv \sqrt{(F^{-1})_{22}}$ for all three methods. For each of the two approximate methods, the right panel shows the fractional difference between the approximate and full Fisher calculations:

$$\frac{\delta\sigma_B}{\sigma_B} = \frac{\sigma_B^{(\mathrm{approx})} - \sigma_B^{(\mathrm{Fisher})}}{\sigma_B^{(\mathrm{Fisher})}}. \tag{4.6}$$

2. *Systematic errors*

Suppose that there is a systematic error, such as a gain error or a rotation error, in one of the antennas of our interferometer. As described in Section II D, we assume that this error can be characterized by an unknown parameter p. For instance, in the case of a gain error, the unknown true gain is $(1+p)$ times the nominal gain, and for a rotation error p is the angle by which the polarizers are misaligned. We treat p as an additional parameter to be estimated, leading to a 3×3 augmented Fisher matrix, whose rows and columns correspond to θ_E, θ_B, p. For example, if we introduce a 10% gain error ($p = 0.1$) to the sixth antenna of the array, the Fisher matrix (4.4) and its inverse (4.5) are replaced by

$$F_{\mathrm{aug}} = \begin{pmatrix} 179 & 4.23 & 8.08 \\ 4.23 & 3.08 & 0.294 \\ 8.08 & 0.294 & 101 \end{pmatrix} \tag{4.7}$$

$$F_{\mathrm{aug}}^{-1} = \begin{pmatrix} 0.00579 & -0.00791 & -0.000439 \\ -0.00791 & 0.33588000 & -0.000346 \\ -0.000439 & -0.000346 & 0.00993 \end{pmatrix} \tag{4.8}$$

We see that the existence of this gain error increases the variance σ_B^2 for about 0.0036%.

Figure 5 shows the effect of a 10% gain error in the sixth antenna, according to the three methods. The quantity plotted is $(\delta\sigma_B^2/\sigma_B^2)^{1/2}$, where $\delta\sigma_B^2 = (\sigma_B^2)_{\mathrm{sys}} - (\sigma_B^2)_{\mathrm{no\ sys}}$ is the difference in the variances of the estimates of B power with and without the systematic error.

C. Gain and rotation errors

Figure 6 shows sample results of the systematic error calculations based on the full Fisher matrix calculation. The left panel shows the additional error induced by a gain error in the sixth antenna as a function of array size N_a, for four different values of the rms gain error σ_p. The right panel shows the same results for a rotation error in the third antenna. In this case, the error parameter p is the angle through which the polarizer has been rotated in radians. In both cases, the noise level is set to 0.0002 μK.

In these sample results, we assumed an error that affected a single antenna, but in a realistic experiment, we would expect all antennas to be affected. The rigorous way to deal with this is to parameterize each of the systematic, build a large augmented Fisher matrix, and calculate σ_B from the resulting matrix. However, it is more convenient if we can treat each systematic error separately and add up the resulting σ_B's. The validity of this approach, of course, depends on the accuracy of treating the individual errors as independent.

Figure 7 shows the results of tests of this independence assumption. For an array with $N_a = 5$ and $n = 0.0002\,\mu$K, we calculated the effects of a 10% gain error in each of the 25 antennas. We also calculated the effect of simultaneous gain errors in each antenna pair. The quantity plotted is the difference between the simultaneous treatment and the quadrature sum of the

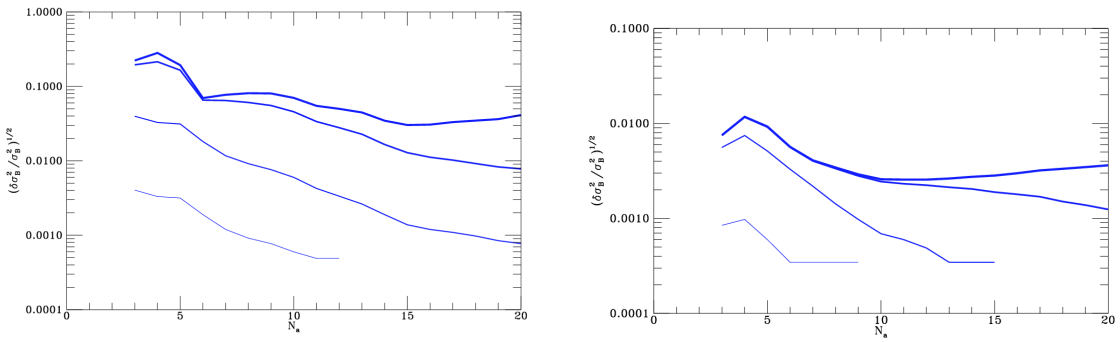

FIG. 6: The additional error caused by a gain error in the sixth antenna (left) and a rotation error in the third antenna (right). From bottom to top, the curves correspond to error levels $\sigma_p = 0.01, 0.1, 1, 10$.

individual errors, specifically

$$\Delta_{ij} \equiv \frac{(\delta\sigma_B^2)_{ij} - ((\delta\sigma_B^2)_i + (\delta\sigma_B^2)_j)}{(\delta\sigma_B^2)_i + (\delta\sigma_B^2)_j}, \qquad (4.9)$$

where i, j label antennas and $\delta\sigma_B^2$ is the additional variance induced by the given error.

The right panel shows the equivalent results for a rotation error of 0.1 rad.

In both cases, the smallness of Δ_{ij} indicates that treating the errors as independent is a good approximation, although the case of rotation errors is not as good as that of gain errors.

V. DISCUSSION

We have presented a Fisher-matrix formalism for assessing the errors on power spectrum estimates from intereferometric measurements of CMB polarization, including the effects of systematic errors. This method occupies an intermediate position between crude analytic approximations [26] and more accurate but far more computationally intensive end-to-end simulations [21–23]. Although detailed simulations are necessary in the end, a fast semianalytic approach such as ours is likely to be useful during the early, exploratory phase of instrument design and optimization.

We have tested our method in a variety of ways, focusing particularly on systematic errors in antenna gain and in the orientation of polarizers of an antenna. Other sources of error can be treated in a similar way. In the absence of systematic errors, our calculations agree with those of simple analytic approximations. The agreement is less good when systematic errors are included (see Fig. 5), which is not surprising given the crudeness of the approximations in the analytic method.

Most of our test results involve errors in a single antenna. Assuming different sources of error are independent, one expects the errors to add in quadrature. We verified for gain and rotation errors that this is a good assumption. In any case, it is not difficult to apply our formalism to the treatment of multiple errors simultaneously.

Because our tests were designed to illustrate the formalism, several idealization were made. We considered a single pointing of the instrument, without including sky rotation or mosaicking [34]. In addition, we assumed a single band power was to be estimated in each of the E and B power spectra. Finally, the errors we considered all involve only E-B mixing, without contamination from the temperature anisotropy. There is no reason that our method cannot be extended to include these and other effects.

Although we developed the method for interferometric CMB polarimetry, the formalism developed herein can be applied to a variety of experiments. In particular, it would be very interesting to consider application to 21-cm tomography, which similarly involves extraction of small fluctuations signals from interferometric visibilities. Computationally expensive simulations are often done to assess the sensitivity of such instruments (*e.g.*, [41]), but a faster semianalytic approach may be valuable as well.

Acknowledgments

This work was supported by NSF Awards AST-1410133 and AST-0908319, and by a Summer Fellowship from the University of Richmond School of Arts and Sciences.

[1] W. Hu, Annals of Physics **303**, 203 (2003), astro-ph/0210696.

[2] A. Challinor, in *IAU Symposium*, edited by M. G. Bur-

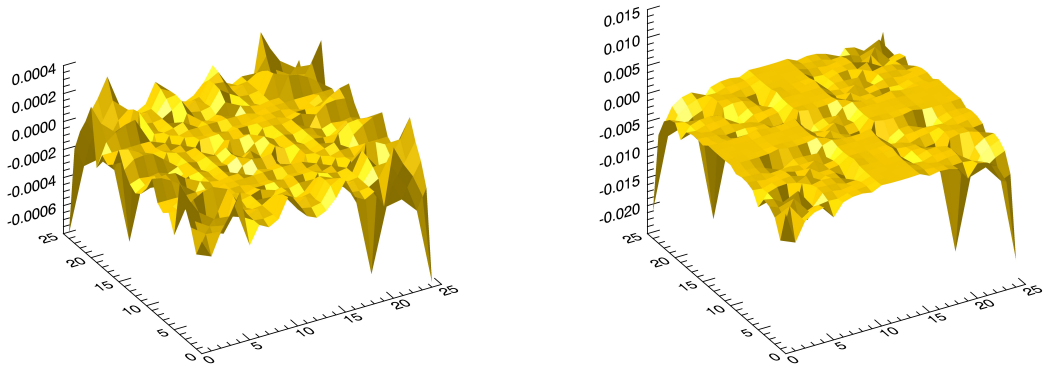

FIG. 7: The inaccuracy caused by treating simultaneous errors in two antennas as if they were independent. The horizontal axes are the antennas of a 5×5 array. The vertical axi is the quantity Δ_{ij} of equation (4.9).

ton, X. Cui, and N. F. H. Tothill (2013), vol. 288 of *IAU Symposium*, pp. 42–52, 1210.6008.

[3] M. Zaldarriaga and U. Seljak, Phys. Rev. D **55**, 1830 (1997), astro-ph/9609170.

[4] U. Seljak and M. Zaldarriaga, Physical Review Letters **78**, 2054 (1997), astro-ph/9609169.

[5] M. Kamionkowski, A. Kosowsky, and A. Stebbins, Physical Review Letters **78**, 2058 (1997), astro-ph/9609132.

[6] M. Kamionkowski, A. Kosowsky, and A. Stebbins, Phys. Rev. D **55**, 7368 (1997), astro-ph/9611125.

[7] A. Lewis, A. Challinor, and N. Turok, Phys. Rev. D **65**, 023505 (2002).

[8] E. F. Bunn, Phys. Rev. D **65**, 043003 (2002).

[9] E. F. Bunn, Phys. Rev. D **66**, 069902(E) (2002).

[10] E. F. Bunn, M. Zaldarriaga, M. Tegmark, and A. de Oliveira-Costa, Phys. Rev. D **67**, 023501 (2003).

[11] E. F. Bunn, Phys. Rev. D **83**, 083003 (2011), 1008.0827.

[12] J. Kim, Astron. Astrophys. **531**, A32 (2011), 1010.2636.

[13] J. Bowyer, A. H. Jaffe, and D. I. Novikov, ArXiv e-prints (2011), 1101.0520.

[14] A. Lewis, Phys. Rev. D **68**, 083509 (2003), astro-ph/0305545.

[15] C.-G. Park and K.-W. Ng, Astrophys. J. **609**, 15 (2004), astro-ph/0304167.

[16] K. M. Smith, Phys. Rev. D **74**, 083002 (2006), astro-ph/0511629.

[17] K. M. Smith, New Astron. Rev. **50**, 1025 (2006), astro-ph/0608662.

[18] K. M. Smith and M. Zaldarriaga, Phys. Rev. D **76**, 043001 (2007), astro-ph/0610059.

[19] L. Cao and L.-Z. Fang, Astrophys. J. **706**, 1545 (2009), 0910.4697.

[20] W. Zhao and D. Baskaran, Phys. Rev. D **82**, 023001 (2010), 1005.1201.

[21] A. Karakci, P. M. Sutter, L. Zhang, E. F. Bunn, A. Korotkov, P. Timbie, G. S. Tucker, and B. D. Wandelt, Astrophys. J. Supp. **204**, 10 (2013), 1209.2930.

[22] L. Zhang, A. Karakci, P. M. Sutter, E. F. Bunn, A. Korotkov, P. Timbie, G. S. Tucker, and B. D. Wandelt, Astrophys. J. Supp. **206**, 24 (2013), 1209.2676.

[23] A. Karakci, L. Zhang, P. M. Sutter, E. F. Bunn, A. Korotkov, P. Timbie, G. S. Tucker, and B. D. Wandelt, Astrophys. J. Supp. **207**, 14 (2013), 1302.6608.

[24] P. M. Sutter, B. D. Wandelt, and S. S. Malu, Astrophys. J. Supp. **202**, 9 (2012), 1109.4640.

[25] W. Hu, M. M. Hedman, and M. Zaldarriaga, Phys. Rev. D **67**, 043004 (2003).

[26] E. F. Bunn, Phys. Rev. D **75**, 083517 (2007), astro-ph/0607312.

[27] A. C. S. Readhead, S. T. Myers, T. J. Pearson, J. L. Sievers, B. S. Mason, C. R. Contaldi, J. R. Bond, R. Bustos, P. Altamirano, C. Achermann, et al., Science **306**, 836 (2004), astro-ph/0409569.

[28] E. M. Leitch, J. M. Kovac, N. W. Halverson, J. E. Carlstrom, C. Pryke, and M. W. E. Smith, Astrophys. J. **624**, 10 (2005), astro-ph/0409357.

[29] M. P. Hobson, A. N. Lasenby, and M. Jones, M.N.R.A.S. **275**, 863 (1995).

[30] M. P. Hobson and J. Magueijo, M.N.R.A.S. **283**, 1133 (1996), astro-ph/9603064.

[31] M. White, J. E. Carlstrom, M. Dragovan, and W. L. Holzapfel, Astrophys. J. **514**, 12 (1999), astro-ph/9712195.

[32] M. P. Hobson and K. Maisinger, M.N.R.A.S. **334**, 569 (2002), astro-ph/0201438.

[33] S. T. Myers, C. R. Contaldi, J. R. Bond, U.-L. Pen, D. Pogosyan, S. Prunet, J. L. Sievers, B. S. Mason, T. J. Pearson, A. C. S. Readhead, et al., Astrophys. J. **591**, 575 (2003), astro-ph/0205385.

[34] E. F. Bunn and M. White, ArXiv Astrophysics e-prints (2006), astro-ph/0606454.

[35] M. Piat, E. Battistelli, A. Baù, D. Bennett, L. Bergé, J.-P. Bernard, P. de Bernardis, M.-A. Bigot-Sazy, G. Bordier, A. Bounab, et al., Journal of Low Temperature Physics **167**, 872 (2012).

[36] A. Ghribi, J. Aumont, E. S. Battistelli, A. Bau, B. Bélier, L. Bergé, J.-P. Bernard, M. Bersanelli, M.-A. Bigot-Sazy, G. Bordier, et al., Journal of Low Temperature Physics **176**, 698 (2014), 1307.5701.

[37] J. R. Pritchard and A. Loeb, Reports on Progress in Physics **75**, 086901 (2012), 1109.6012.

[38] M. F. Morales and J. S. B. Wyithe, Ann. Rev. Astron. Astrophys. **48**, 127 (2010), 0910.3010.

[39] J. O. Berger, *Statistical Decision Theory and Bayesian*

Analysis (Springer, 1993), 2nd ed.

[40] Planck Collaboration, P. A. R. Ade, N. Aghanim, C. Armitage-Caplan, M. Arnaud, M. Ashdown, F. Atrio-Barandela, J. Aumont, C. Baccigalupi, A. J. Banday, et al., Astron. Astrophys. **571**, A16 (2014), 1303.5076.

[41] L. Zhang, E. F. Bunn, A. Karakci, A. Korotkov, P. M. Sutter, P. T. Timbie, G. S. Tucker, and B. D. Wandelt, ArXiv e-prints (2015), 1505.04146.

Appendix A: The detailed form of the visibility covariance matrix

We assume a Gaussian antenna pattern as in equation (2.5),

$$A(\mathbf{r}) = e^{-\mathbf{r}^2/2b^2} \tag{2.5}$$

whose Fourier transform is

$$\tilde{A}(\mathbf{k}) = \tilde{A}^*(\mathbf{k}) = \frac{b^2}{2\pi} e^{-b^2\mathbf{k}^2/2}, \tag{A1}$$

Substituting this into equation (2.41), we find

$$\begin{aligned}
&\langle V_Q(\mathbf{u}_1) V_Q^*(\mathbf{u}_2)\rangle \\
&= (2\pi)^2 \int \left[P_E(\mathbf{k})\cos^2(2\phi) + P_B(\mathbf{k})\sin^2(2\phi)\right] \\
&\quad \tilde{A}^*(\mathbf{k}+2\pi\mathbf{u}_1)\tilde{A}(\mathbf{k}+2\pi\mathbf{u}_2) d^2\mathbf{k}
\end{aligned} \tag{2.41}$$

Then

$$\begin{aligned}
&\langle V_Q(\mathbf{u}_1) V_Q^*(\mathbf{u}_2)\rangle \\
&= b^4 \int \left[P_E(\mathbf{k})\cos^2(2\phi) + P_B(\mathbf{k})\sin^2(2\phi)\right] \\
&\quad \exp\left[-\frac{1}{2}b^2\left[(\mathbf{k}+2\pi\mathbf{u}_1)^2 + (\mathbf{k}+2\pi\mathbf{u}_2)^2\right]\right] d^2\mathbf{k} \\
&= b^4 \int \left[P_E(k)\cos^2(2\phi) + P_B(k)\sin^2(2\phi)\right] \\
&\quad \exp\big[-b^2\left[2\pi^2(u_1^2+u_2^2)+k^2\right] - 2\pi b^2 \\
&\quad \left[(u_{1x}+u_{2x})k\cos\phi + (u_{1y}+u_{2y})k\sin\phi\right]\big] k dk d\phi.
\end{aligned} \tag{A2}$$

For convenience, we make the following definitions:

$$\begin{aligned}
S_1(k) &= \int_0^{2\pi} \cos^2(2\phi) \\
&\exp\left[-2\pi b^2\left[(u_{1x}+u_{2x})k\cos\phi + (u_{1y}+u_{2y})k\sin\phi\right]\right] d\phi,
\end{aligned} \tag{A3}$$

$$\begin{aligned}
S_2(k) &= \int_0^{2\pi} \sin^2(2\phi) \\
&\exp\left[-2\pi b^2\left[(u_{1x}+u_{2x})k\cos\phi + (u_{1y}+u_{2y})k\sin\phi\right]\right] d\phi,
\end{aligned} \tag{A4}$$

$$\begin{aligned}
S_3(k) &= \int_0^{2\pi} \sin(4\phi) \\
&\exp\left[-2\pi b^2\left[(u_{1x}+u_{2x})k\cos\phi + (u_{1y}+u_{2y})k\sin\phi\right]\right] d\phi,
\end{aligned} \tag{A5}$$

and

$$q(x) = \exp\left[-b^2[2\pi^2(u_1^2+u_2^2)+k^2]\right]. \tag{A6}$$

Then one can check that

$$\begin{aligned}
\langle V_Q(\mathbf{u}_1) V_Q^*(\mathbf{u}_2)\rangle &= b^4 \int_0^\infty P_E(k) q(k) S_1(k) k dk \\
&\quad + b^4 \int_0^\infty P_B(k) q(k) S_2(k) k dk.
\end{aligned} \tag{A7}$$

Similarly, for the U-U and Q-U covariance matrix elements,

$$\begin{aligned}
\langle V_U(\mathbf{u}_1) V_U^*(\mathbf{u}_2)\rangle &= b^4 \int_0^\infty P_B(k) q(k) S_1(k) k dk \\
&\quad + b^4 \int_0^\infty P_E(k) q(k) S_2(k) k dk.
\end{aligned} \tag{A8}$$

$$\begin{aligned}
\langle V_Q(\mathbf{u}_1) V_U^*(\mathbf{u}_2)\rangle &= -\frac{1}{2} b^4 \int_0^\infty P_E(k) q(k) S_3(k) k dk \\
&\quad + \frac{1}{2} b^4 \int_0^\infty P_B(k) q(k) S_3(k) k dk.
\end{aligned} \tag{A9}$$

Equations (A7), (A8), and (A9), combined with equations (A3), (A4), (A5), and (A6), are sufficient to present a workable algorithm to calculate the visibility covariance matrix. We now provide the analytic forms of the integrals S_1, S_2, and S_3 as the ending of this section. We will take S_1 as an example and directly give S_2 and S_3.

Let

$$a = (u_{1x}+u_{2x})k, \tag{A10}$$

$$b = (u_{1y}+u_{2y})k. \tag{A11}$$

Then

$$S_1(k) = \int \cos^2(2\phi) \exp\left[-2\pi b^2(a\cos\phi + b\sin\phi)\right] d\phi. \tag{A12}$$

Now let

$$t = \arctan\frac{b}{a}, \tag{A13}$$

$$\theta = \phi + t, \tag{A14}$$

$$l = \sqrt{a^2+b^2}. \tag{A15}$$

Then

$$\begin{aligned}
S_1(k) &= \int \cos^2(2\theta - 2t) \exp\left[-2\pi b^2 l \sin\theta\right] d\theta \\
&= \int \cos^2(2\theta)\cos^2(2t)\exp(-2\pi b^2 l\sin\theta) d\theta \\
&\quad + \int \sin^2(2\theta)\sin^2(2t)\exp(-2\pi b^2 l\sin\theta) d\theta.
\end{aligned} \tag{A16}$$

Define

$$S_{11}(k) = \int \cos^2(2\theta) \exp(-2\pi b^2 l \sin\theta) d\theta, \tag{A17}$$

$$S_{12}(k) = \int \sin^2(2\theta) \exp(-2\pi b^2 l \sin\theta) d\theta. \tag{A18}$$

Then

$$S_1(k) = S_{11}(k)\cos^2(2t) + S_{12}(k)\sin^2(2t). \tag{A19}$$

The integrals S_{11} and S_{12} can be written analytically using the modified Bessel function of the first kind $I_n(x)$:

$$S_{11}(k) = \frac{2}{l^3\pi^2 b^6}\big[l\pi b^2(3 + l^2\pi^2 b^4) I_0(2l\pi b^2) - (3 + 2l^2\pi^2 b^4) I_1(2l\pi b^2)\big], \tag{A20}$$

and

$$S_{12}(k) = \frac{2}{l^2\pi b^4}\big[2l\pi b^2 I_1(2l\pi b^2) - 3I_2(2l\pi b^2)\big]. \tag{A21}$$

We can follow the similar reasoning to calculate S_2 and S_3. The results are

$$S_2(k) = S_{11}(k)\sin^2(2t) + S_{12}(k)\cos^2(2t), \tag{A22}$$

and

$$S_3(k) = -\frac{2\sin(4t)}{l^3\pi^2 b^6}\big[l\pi b^2(6 + l^2\pi^2 b^4) I_0(2l\pi b^2) - 2(3 + 2l^2\pi^2 b^4) I_1(2l\pi b^2)\big]. \tag{A23}$$